

Influence of Acquisition Parameters on Pigment Classification using Hyperspectral Imaging

Dipendra J. Mandal, Sony George, and Marius Pedersen[▲]

Department of Computer Science, Norwegian University of Science and Technology (NTNU), Norway
E-mail: dipendra.mandal@ntnu.no

Clotilde Boust

Centre de Recherche et de Restauration des Musées de France (C2RMF), & CNRS PCMTH PSL

Abstract. *Pigment classification of paintings is considered an important task in the field of cultural heritage. It helps to analyze the object and to know its historical value. This information is also essential for curators and conservators. Hyperspectral imaging technology has been used for pigment characterization for many years and has potential in its scientific analysis. Despite its advantages, there are several challenges linked with hyperspectral image acquisition. The quality of such acquired hyperspectral data can be influenced by different parameters such as focus, signal-to-noise ratio, illumination geometry, etc. Among several, we investigated the effect of four key parameters, namely focus distance, signal-to-noise ratio, integration time, and illumination geometry on pigment classification accuracy for a mockup using hyperspectral imaging in visible and near-infrared regions. The results obtained exemplify that the classification accuracy is influenced by the variation in these parameters. Focus distance and illumination angle have a significant effect on the classification accuracy compared to signal-to-noise ratio and integration time. © 2021 Society for Imaging Science and Technology.*

[DOI: 10.2352/J.ImagingSci.Technol.2021.65.5.050406]

1. INTRODUCTION

Hyperspectral Imaging (HSI), also called imaging spectroscopy, is a non-invasive imaging technique that generates a spatial map over continuous spectral bands, producing a three-dimensional datacube i.e., two spatial and one spectral dimension. On the basis of data acquisition methods, a spectral data can be created using three general approaches namely, whiskbroom (point scanning), pushbroom (line scanning), and snapshot (single-shot). The line scanning approach is widely adopted because of its higher Signal-to-Noise Ratio (SNR) and flexibility [1]. In this approach, the object is scanned line by line at a time, it uses an array of detectors to scan over a two-dimensional surface using a detector perpendicular to the surface of an object being scanned [2, 3]. HSI technology which was initially developed and used for remote sensing applications [4] has later been used in different application domains such as agriculture [5], medical [6], forensic [7], biomedical engineering [8],

Cultural Heritage (CH) [9], etc. Materials with distinct spectra as each element emits a distinctive set of discrete wavelengths according to its atomic and molecular electronic structure [10].

With the development of sophisticated hardware and software, this imaging technology is being used more frequently for the analysis of work of art [11, 12]. Pigment classification of artwork materials such as paintings is of importance for conservators to do a precise analysis of an object and understand its historical value [13, 14]. Despite the significant utilization of HSI in this field [15–18], there are still important challenges in terms of delivering high-quality spectral data. Defining image quality is a complex subject. For three-channel (RGB) imaging, quality criteria are often subjective as it reflects the visual perception of a human observer [19, 20]. However, for HSI it is not only limited to perceptual quality, as it captures data beyond the visible range and is used for a wide range of applications, therefore it is difficult to generalize the definition of quality. Several definitions of spectral quality can be found in the literature and most of them depend upon the application. Fryskowska et al. [21] define quality as the suitability of a specific dataset for a specific purpose. This is more appropriate for spectral imaging in general and thus for pigment classification, the obtained spectral data will be considered to have high quality if the classification accuracy is high. From the perspective of image quality in spectral imaging, most of the research work has been focused on the remote sensing application [22], where the acquisition is made from satellites and aircrafts with significant ground sample distance. The sun is a primary source of illumination; the scattering and absorption of sunlight by different layers of the atmosphere can result in intensity modifications and spectral variations, resulting in degradation of obtained data quality. To deal with such degradation, many algorithms have been developed, for example, correction of atmospheric interference [23]. However, for CH applications, the acquisition is carried out in a close range and the quality of obtained data depends upon parameters of the HSI system such as illumination geometry, the focus of optics, sensor integration time, and SNR [18, 24]. Although instrument calibration is an essential step to obtain valuable and relevant results from HSI, however, more of these parameters are quantified by

[▲] IS&T Member.

Received June 4, 2021; accepted for publication Sept. 21, 2021; published online Oct. 14, 2021. Associate Editor: Markku Hauta-Kasari.

1062-3701/2021/65(5)/050406/13/\$25.00

device manufacturers and, therefore, are not considered in this paper.

In an artwork, the pigments used are usually mixed, i.e., one or more pigments are mixed with a binder such as oil, egg tempera, gum, etc., and therefore have heterogeneous structures that can have a significant effect on gloss levels. For example, mixture of some pigments, or paintings with varnish layers can cause specular reflection, especially due to the angle of illuminations [25], which will further affect the spectral accuracy and result in incorrect pigment classification. The illumination used is an important factor in imaging. A study done by Toque et al. [26] showed that the spectral reflectance obtained using multispectral imaging of a painting was influenced by the lighting conditions. Intensity, type of illumination, and angle of incidence were key elements that influence the resulting data. In a painting, surfaces are often uneven, therefore acquiring images at an optimal focus distance can be a difficult task. Hence, it is important to explore how this influences the obtained spectral data and classification accuracy.

In CH applications, objects are sensitive to temperature. Any object exposed to an illuminant for a longer time during acquisition can result in a change in the material property due to the heat generated by the illuminant, causing significant damage to the object. One possible way to minimize this effect is by increasing the speed of the acquisition. Higher integration time also increases the noise level in the data. It is very common to use silicon-based detectors, such as a charge-coupled device (CCD) in VNIR HSI systems. Such sensors have lower sensitivity at the two ends of wavelength in the VNIR region, i.e. near 400 and 1000 nanometers (nm), resulting in a noisy spectrum in this region. Thus, it is important to investigate how the reconstructed spectrum of artwork materials differs from their original when there is variation in imaging parameters. Therefore, the objective of this research work is to investigate the effect of imaging parameters such as focus, integration time, SNR, and illumination geometry on the classification accuracy of pigments. The rest of this paper is structured as follows, Section 2 describes the state of the art for image acquisition parameters, and it summarizes how these parameters can affect the overall quality when used with the HSI systems for CH applications. Object details, imaging technology, and the experimental framework used are stated in Section 3. Section 4 covers the result with discussions. Finally, Section 5 presents conclusions followed by future work.

2. STATE OF THE ART

In a digital imaging system, the acquisition stage can be considered as an essential component. For acquisition of high-quality digital data, several acquisition parameters need to be addressed and controlled. Digital image capture is a function of the light source, reflective surface, distance, the angle between the device, the surface, and the illuminant. The optical resolution, noise, depth of field, integration time, illumination, etc. are some of the important acquisition

parameters [27, 28]. These parameters are linked to quality attributes such as sharpness, color, tonality, and resolution, and can influence the overall quality of the captured data. In an imaging device with a low depth of field, the objects at different depths from the camera may appear out of focus if they are away from the focus plane [29, 30]. When capturing CH objects, it should be a sharp focus across the entire object being captured, but depending upon the depth of field and object irregularities, it can result in variation in image sharpness resulting in a blurry image and consequently degrading the quality [31].

Illumination is an important factor that often influences image quality attributes such as color reproduction and texture. During an acquisition, if the object is overexposed, the image will be brighter, and the details of the highlights in the scene will be lost, while on the other hand if the exposure is insufficient, the details in the shadows of the scene will be difficult to distinguish. Loss of image details can reduce the usefulness of the acquired images in CH documentation. Accurate color reproduction is an essential requirement for documentation and study of artworks [32–34] e.g., monitoring the fading phenomena and studying color change due to removal of the varnish layer [35, 36]. Image acquisition parameters mentioned above can be more or less important depending upon the application and objective of imaging. Different imaging technologies can be used for image acquisition, allowing more or less similar acquisition parameters. These imaging technologies can be grouped in multi-band, multispectral, and hyperspectral depending on the number of bands selected over a given spectral interval and on their bandwidths.

Numerous studies have shown the successful use of HSI in the study and analysis of CH artefacts [9, 25, 37, 38]. However, the image acquisition of artworks using HSI has several issues for acquiring high-quality data [39–41] and it involves a number of calibrations and corrections steps to obtain an accurate spectral data [24, 42, 43]. Kubic et al. [25] discussed some problems of HSI acquisition of a painting. Depth of field is also crucial for close-range HSI, particularly for artwork such as paintings that are often warped or have uneven surfaces. Thus, acquiring spectral data at the optimum focus can be challenging. Qureshi et al. [41] discussed few challenges involved in the acquisition and processing of HSI for documents. SNR, integration time, and illumination are the most highlighted imaging parameters that influence the quality of HSI data. Pillay et al. [24] have addressed similar parameters and the usefulness of filters, such as equalization and polarizing filters, in the HSI acquisition workflow that can affect the overall data quality.

To gain a better understanding of spectral imaging devices and analyze how they influence data reliability for different artworks, working group 1 of the EU COST-Action TD1201, Color and Space in Cultural Heritage (COSCH) (website: <http://www.cosch.info/>) initiated a round-robin test that was carried out by nineteen institutions across Europe for five different types of objects using both multispectral and HSI [17]. It addresses various issues related

to instrumentation, data collection, and post-processing over the accuracy and reliability of data. The resulting data was affected (error in spectral alignment, noise, spatial distortion, etc.) by various aspects, such as device configuration, acquisition environment, and methods of data processing, and this could further have an important effect on pigment classification. MacDonald et al. [44] performed a quality assessment of Russian icon digitization, it was one among five different objects used in the COSCH project. They found that the obtained data was degraded due to specular reflections from both glossy painted and metallic gold areas of the icon's surface indicating the control over the illumination geometry. The imaging system used and workflows employed by the participating institutions varied widely, including camera specifications, illumination, imaging geometry, and file formats. It also highlighted that there is a strong need of guidelines for the spectral imaging workflow.

Generally, halogen lamps are used as an illumination source due to their continuous spectrum of light, from ultraviolet to mid-infrared region, i.e., 350–3400 nm. Halogen lamps emit significant levels of electromagnetic radiation, a lot of energy is converted into heat. Organic materials are more sensitive to heat, moderate heat can change the properties of varnish affecting the glossiness of an object. Artwork exposed under excessive heat for a longer time can have a destructive impact, for instance, melting of the varnish or even the paint layer [45]. This can be minimized by following the guidelines, which suggest the use of a proper illumination level (150–200 lux for oil paintings and 50 lux for manuscripts and other paper-based artworks) and other environmental factors for sensitive CH objects [46, 47]. An illumination source that raises the surface temperature of an object more than four degrees Fahrenheit (257.6 K) in the total acquisition process, is not recommended [48]. Fundamentally light-induced damage is determined by the accumulated total energy incident on material i.e. lux hour rather than the intensity of the incident light. Illumination used in an imaging device setup for an art object can be used either with low-intensity light for a longer time or with high-intensity light for a short time; in both conditions, we may achieve similar SNR. Nevertheless, this reciprocity principle might not always hold for every work of art, for example, some pigments in a painting, and can be independent of time period [49]. However, due to the total energy incident on an object, higher intensity light is preferred [38].

Whetton et al. [50] evaluated the effect of camera height, angle, integration time, and distance between the illuminant and the object on the SNR for wheat plant canopy captured with an HSI system and found these parameters to have a high influence on the spectral quality. A noisy spectrum was obtained when imaged with low integration time and a larger distance between an illuminant and the object. Due to the acquisition setup similarity (i.e., close range), we assume these parameters might also influence the acquisition of CH applications. Likewise, Wang et al. [51] also mentioned focus and integration time as factors influencing spectral image quality. For acquisition of images of fruits using HSI, it was

difficult to preserve the focus due to nonuniform fruit size (parameters comparable to CH objects), resulting in either too bright or too dark areas within the fruits making feature extraction a difficult task. To solve this issue, the author recommended a few steps such as changing the orientation of scanning, adding additional lamps, and using a multi-step reflectance target.

Researchers often prepare mockups using specific pigments mixed using binders [52, 53]. These are modern pigments having similar properties to historical pigments from different periods. Generally, shiny materials were used in traditional Asian arts and imaging such objects often causes serious challenges as the intensity of the specular reflection component is usually much higher than that of the diffuse reflection, producing a saturated image. Light scattering is dependent upon the surface properties such as roughness, reflective binders, varnishes, etc., and can modify the spectral reflectance behavior [54, 55], it can also cause specular reflection especially on varnished or glossy paintings. Even in controlled laboratory conditions, non-homogeneously illuminated paintings result in highlights and shadowy areas and degrade the overall quality below a useful level.

In artwork analysis, one of the important tasks is pigment identification [26, 38, 56, 57]. For pigment classification using HSI, the two common approaches are supervised and unsupervised methods. Researchers mostly use supervised classification [58, 59], where they compare the obtained spectrum with a reference spectrum that is mostly created within a Region Of Interest (ROI) and stored as a spectral library, whereas, in an unsupervised method, it looks for spectral clustering of pixels [59, 60]. One of the most commonly applied classification algorithms using data from HSI is the Spectral Angle Mapper (SAM) [61, 62]. This method considers the angle formed between the spectrum of the reference and the test image at each pixel, where smaller angles represent a closer match of the spectrum. Each spectrum is treated as a vector in an N -dimensional space where N is equal to the number of spectral bands. Few other algorithms used for supervised classification are spectral correlation mapper [62], maximum likelihood [63], spectral information divergence [64], and spectral gradient mapper [65]. It is essential to assure that the spectral data acquired from the artwork is accurate to achieve the precise classification of the materials/pigments present in the artwork. The HSI acquisition parameters can influence the quality of the spectral data, and the objective of the presented research is to study the link between them.

3. MATERIALS AND METHODS

In this section, we describe the test object and the hyperspectral image acquisition laboratory setup, followed by details on the acquisition parameters. The classification model and data post-processing steps are also explained.

3.1 Test Object

A pigment mockup [53] was used as a test object in this work. The reason to choose this mockup as an object was because

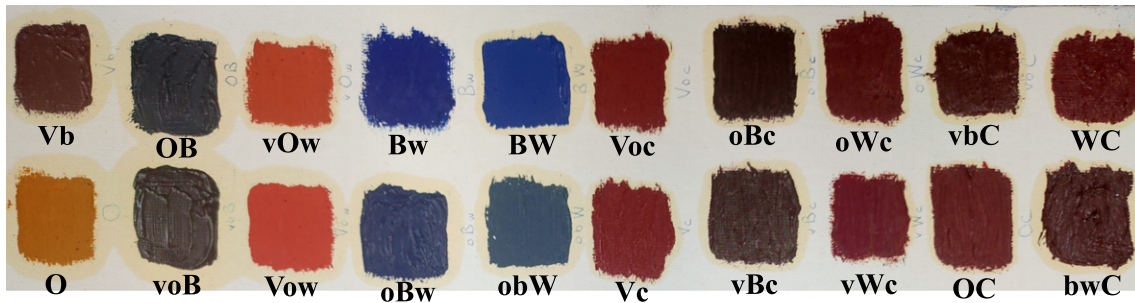


Figure 1. Pigment mockup used as test object. Labels for patches have been added here for description and are not part of the mockup.

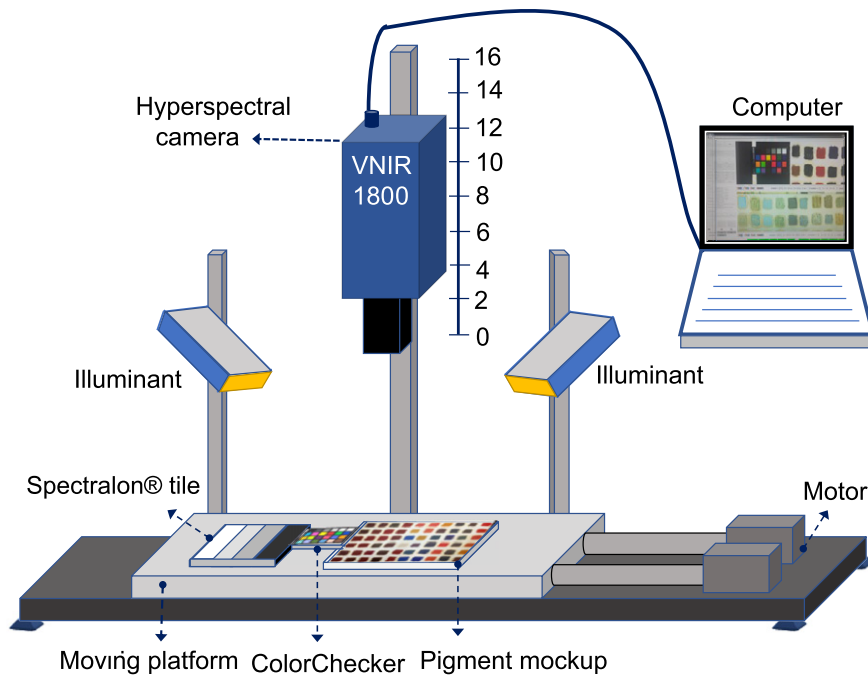


Figure 2. The layout of HSI system used for the experiment. Illumination used was a 150 W halogen-based SmartLite 3900e produced by Illumination Technologies, Inc., guided on the object via optical fiber. Illumination geometry is 45° - 0° - 45° , here 0° implies camera angle with normal.

of its material and physical characteristics considering its usefulness in CH. Powder pigments that are known to have been used in the historic period (14th–18th century) were mixed using linseed oil as a binder and applied over a stretched canvas that were pre-primed using gesso. Patches were made using different concentrations of seven pigments, each weighed on a precision scale. The pigments were Vermilion (V), Ultramarine Blue (B), Viridian Green (G), Naples Yellow (Y), Gold Ochre (O), Kremer White (W), and Novoperm Carmine Red (C). In the remaining part of this paper, we will denote these pigments with their abbreviations. Abbreviations in the capital and small letter will be used to denote the concentration of mixtures. For example, the letter VB denotes that the ratio of mass is 1:1 for pigments B and V. Similarly, Bv is 2:1 and Bvy means 2:1:1. A picture of the pigment mockup is shown in Figure 1.

3.2 Experimental Setup

Hyperspectral images were obtained in a laboratory environment using the line scanner HySpex VNIR-1800 developed by Norsk Electro Optikk [66], consisting of an actively cooled and stabilized complementary metal-oxide-semiconductor detector. The spectral data obtained covers a spectral range from 400 to 1000 nm with 186 spectral bands having a spectral sampling of 3.26 nm. The scanning speed is automatically synchronized with the integration time which is manually set on the device using the camera interface software HySpex GROUND. In this experiment, a 30 cm cylindrical lens was used that captures 1800 spatial pixels across a line with a field of view of approximately 86 mm.

As shown in Figure 2 the experiment was conducted in a laboratory environment and a translation stage setup was used where the pigment mockup was placed on the moving

platform. The Spectralon[®] multi-step reference target [67] consisting of four adjacent panels with reflectance values 99, 50, 25, and 12% and a ColorChecker [68] was also kept along with the test target at the same horizontal level in every scan as shown in Figure 3 and were perpendicular to the focal axis of the camera [69]. The reference target is used for computing the normalized reflectance at the pixel level. The objective of using a ColorChecker was to validate the obtained spectral data.

3.3 Methodology

Setup as shown in Fig. 2, the optimal focus is obtained at a distance of 22 cm from the camera as claimed by the HSI device manufacturer. We will consider this distance as a reference focus point (Gnd_T) throughout this paper. For focus, we choose to change the distance away from the camera with a step size of 2 cm from Gnd_T. Due to the arrangement of the setup, it was convenient to move the camera in the direction as shown in Fig. 2. The Number of scans (N) was changed for pushbroom HSI, which is scanning every single line multiple times and taking an average before moving to the following line. This procedure improves the SNR ratio by a factor of N . For a work of art reducing the measurement time as much as possible reduces the exposure to the radiation during acquisition of HSI data which further helps in safeguarding the analyzed work. Therefore, for SNR, acquisition with a value of N equal to 1, 2, 4, 6, and 8 was carried out and it was done by giving input directly to the software provided by device manufacture. Orientation including other acquisition parameters was kept as specified in Fig. 2.

Integration time is another important attribute of image acquisition. Acquiring an image at a lower integration time will make the acquisition process faster and lower the exposure of an object to the illumination. There is a trade-off between light intensity and integration time, as it is important to keep the art object less exposed to high light intensities. Therefore, for this part of the experiment, we changed the integration time from the minimum (allowed by the device software i.e., 2150 μ s) to a certain higher value (i.e., 12,500 μ s) so that its pixels have saturation values between 85% and 10%. The scanning was conducted with SNR equal to 2. In the last part of the experiment, we studied the influence of illumination angle on the acquired spectral data for classification accuracy. The standard configuration for scanning is at 0°, 45° for the camera and illuminant, respectively. We changed the angle of the illuminant to 30° and 60°.

Detectors have low sensitivity at low and high extremes of the spectral range and the illumination intensities near these regions are weak as well, thus resulting in the adding of noise in the spectral data. One possible way is to use an equalization filter. This helps to improve the SNR mainly towards the extremes of wavelength at the same time it also limits the power efficiency of the light source in the central region of the detector and might need a longer integration time. We used an equalization filter on the device and the acquisition of the pigment mockup was carried out at an



Figure 3. Acquisition arrangement of pigment mockup with the Spectralon[®] multi-step reference target to the left and ColorChecker on the right. Numbering for ColorChecker is added manually here in this figure for reference.

illumination angle of 45° to observe its effect on the obtained spectral data.

3.4 Data Processing

The obtained raw hyperspectral data require post-processing to acquire calibrated normalized reflectance data. Radiometric calibration was carried out where the raw digital number

data from the camera was corrected for non-uniformity and dark offset and then converted to sensor level absolute radiance value using the standalone post-processing software HySpex RAD. Finally, the reflectance factor for the pigment mockup was calculated using the known reflectance value of the reference target. Calculation is shown in Eq. (1), where, $R_{Obj}(\lambda)$ is the reflectance of an object, $R_{Ref_t}(\lambda)$ is the reflectance of reference target, $r_{Obj}(\lambda)$ and r_{Ref_t} are sensor absolute radiance values for the object and reference target, respectively. The reference target surface might have some variation in pixel value, so we averaged the values from 100 pixels for each line scan and calculated the reference target radiance value. Due to the small distance between the sensor and the object, we assumed that the path radiance effect to be negligible. The obtained spectral data was then cropped to exclude the ColorChecker and the reference target. The modification was made using the open-source software Spectralpython [70].

$$R_{Obj}(\lambda) = R_{Ref_t}(\lambda) \frac{r_{Obj}(\lambda)}{r_{Ref_t}(\lambda)} \quad (1)$$

$$\alpha = \cos^{-1} \frac{\sum_{i=1}^{nb} t_i r_i}{\sqrt{\sum_{i=1}^{nb} t_i^2} \sqrt{\sum_{i=1}^{nb} r_i^2}}. \quad (2)$$

For classification, a supervised approach using the SAM algorithm was applied with a default threshold angle of 0.1 radians. The spectral angle between an image pixel and reference spectrum is given by Eq. (2), where α is the spectral angle in radians, t_i is the image spectrum, r_i is the reference spectrum and nb is the total number of bands. We defined the training region for each of the pigment patches, i.e. an ROI of approximate size equal to that of the patches (25×25 mm) was considered, and the regional mean spectrum from these patches were stored and used as the reference spectrum. The classification accuracy was calculated with the statistical parameters, i.e., confusion matrix [71, 72] using the commercial remote sensing software Environment for Visualizing Images (ENVI). The overall methodology is illustrated using a block diagram in Figure 4 and Table I shows the summary of the acquisition parameters.

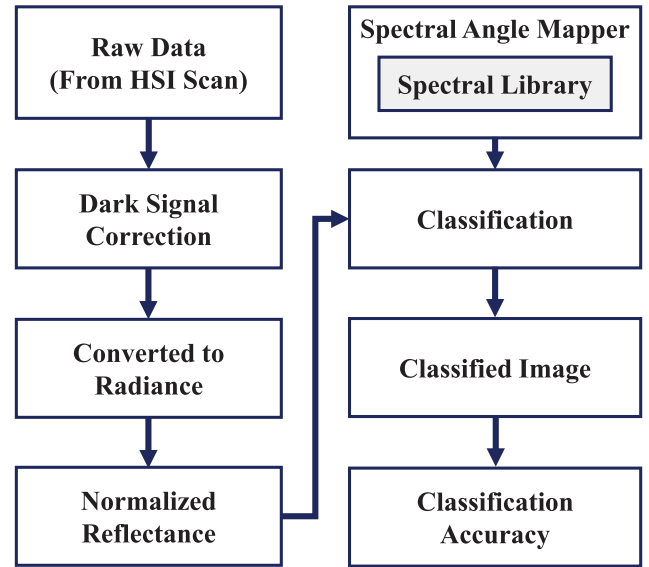


Figure 4. Hyperspectral data processing workflow diagram.

Figure 5(a) shows the pigment patches and Fig. 5(b) illustrates its corresponding image after classification. Different colors in Fig. 5(a) indicate pixels for the particular patch. Accuracy is evaluated as the ratio of classified pixels to the total pixels in a given ROI polygon. As an example, the result of the classification of four patches under optimal acquisition conditions is shown in Table II.

4. RESULTS AND DISCUSSION

In this section, we will look in detail at the spectrum and classification accuracy obtained for the mockup and ColorChecker by varying the quality attributes, i.e. focus, SNR, integration time, and illumination angle.

4.1 Focus

Figure 6 shows the spectrum of three different patches for varying focus distance from 0 cm (Gnd_T) to 16 cm away from the initial position of the camera. For the patch O (Fig. 6a) there are slight changes in the magnitude of the spectrum mainly in the range between 600 and 1000 nm. Whereas for the patch OB (Fig. 6b) and patch voB (Fig. 6c) we can see a spectral variation in both visible and near-infrared regions. The spectrum is plotted for a small region within the given patch, i.e., averaging 10×10 pixels, each patch is

Table I. Acquisition parameters. Variable indicates the different values at which acquisition was done and fixed parameters imply the condition that was constant for each set of experiments; I is illumination measured.

Acquisition parameters	Variables	Fixed parameters
Focus distance (F)	{Gnd_T, 2, 4, 6, 8, 10, 12, 14, 16} cm	SNR = 2, IT = 12,500 μ s, A = 45°, and I = 3200 lux
SNR	{N = 1, 2, 4, 6, 8}	F = Gnd_T, IT = 12,500 μ s, A = 45°, and I = 3200 lux
Integration Time (IT)	{2150, 2500, 5000, 7500, 10,000, 12,500} μ s	F = Gnd_T, SNR = 2, A = 45°, and I = 3200 lux
Illumination Angle (A)	30°, 45° and 60°, and I = 2375, 3200 and 4700 lux	F = Gnd_T, SNR = 2, and IT = 12,500 μ s

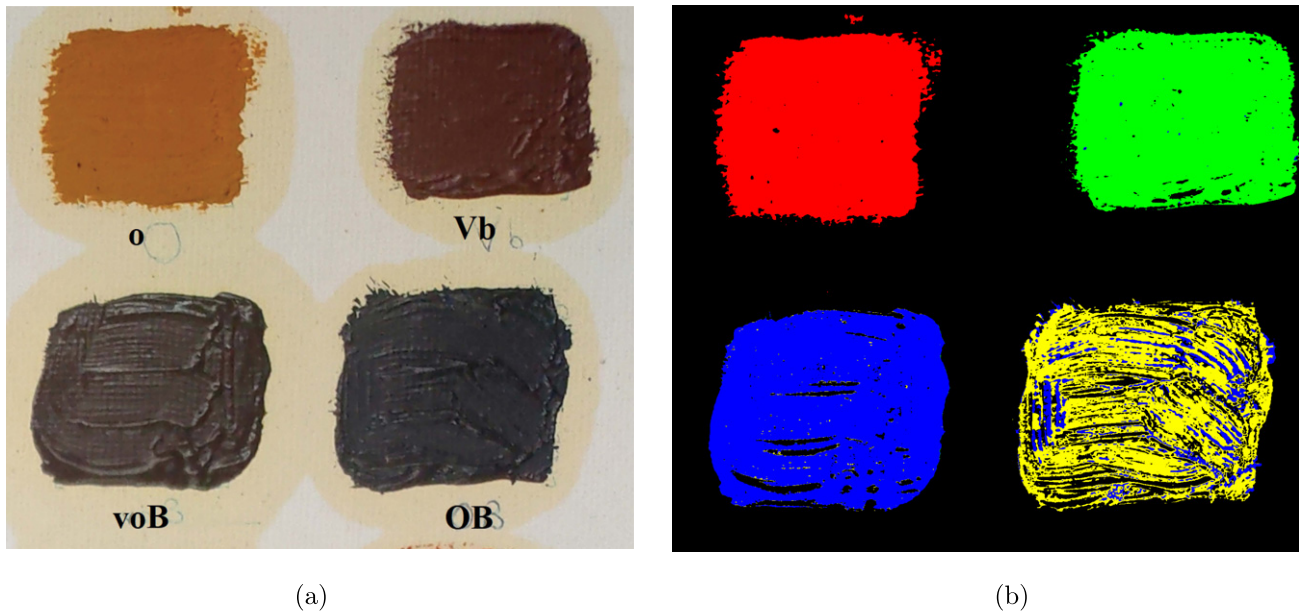


Figure 5. (a) Pigment patches, single pigment O; Vb patch is a mixture of two with concentration 2:1; voB mixture of three with concentration 1:1:2; OB contains two pigments with equal concentration. (b) Classified image, where color indicates the class that each pixel has been classified to.

Table II. Classification accuracy: total number of pixels classified correctly for each patch within the selected ROI.

	Patch O Red	Patch Vb Green	Patch voB Blue	Patch OB Yellow
Patch O (Red)	80,850 (99.98%)	0	0	0
Patch Vb (Green)	0	73,223 (99.90%)	0	0
Patch voB (Blue)	01	0	68,337 (93.40%)	30,739 (33.50%)
Patch OB (yellow)	0	0	2159 (2.95%)	45,812 (49.93%)
Unclassified	14 (0.02%)	74 (0.10%)	2668 (3.65%)	15,209 (16.57%)
Total No. of Pixels	80,864	73,297	73,164	91,760

approximately 500×500 pixels. In general, we can observe that there is a change in the magnitude of the spectrum, and the shape of the spectrum is moreover constant.

It was also seen that variation in magnitude of spectrum change with the number of pixels chosen to average, in fact, data plotted from sub-areas in different places within the same patch showed high variations as shown in Figure 7(a). This is mainly because of variation in pigments mixture concentration and nonuniformity in the applied layers. The effect of this variation and nonuniformity is also seen in classification, as shown in Fig. 5(b), not all patches are equally classified and thus have different classification accuracy. More pixels are classified in patches with a single pigment and or homogeneous texture compared to that of having a rough texture. Liang [38] also mentioned that the ratio of pigment concentration to binding medium affects the peak of the spectrum. This argument can be supported by observing the spectra of ColorChecker patches as shown in Fig. 7(b), we can observe that there is a slight variation in magnitude

towards the higher wavelength but still the overall shape of the spectrum is similar.

The result for the pigment classification overall accuracy for the given mockup is shown in Figure 8. It is observed that the classification accuracy initially increases as an object gets further away from the camera starting from the optimal focus point and after some points, it starts to decrease. It is because as it moves away from an object, pixels become slightly out of focus and therefore blurred (smoothed), and more adjacent pixels are averaged. As the camera moves further away from the pigment mockup, the camera is outside the optimal focus distance and depth of field, thus photons from the pigment patch area are no longer hitting the same pixels and start to hit adjacent pixels and affect the obtained spectrum.

4.2 SNR

Spectrum for various SNR levels (frame averaging) for three different patches are shown in Figure 9. The three patches shown are a patch with a single pigment (Fig. 9a), a mixture

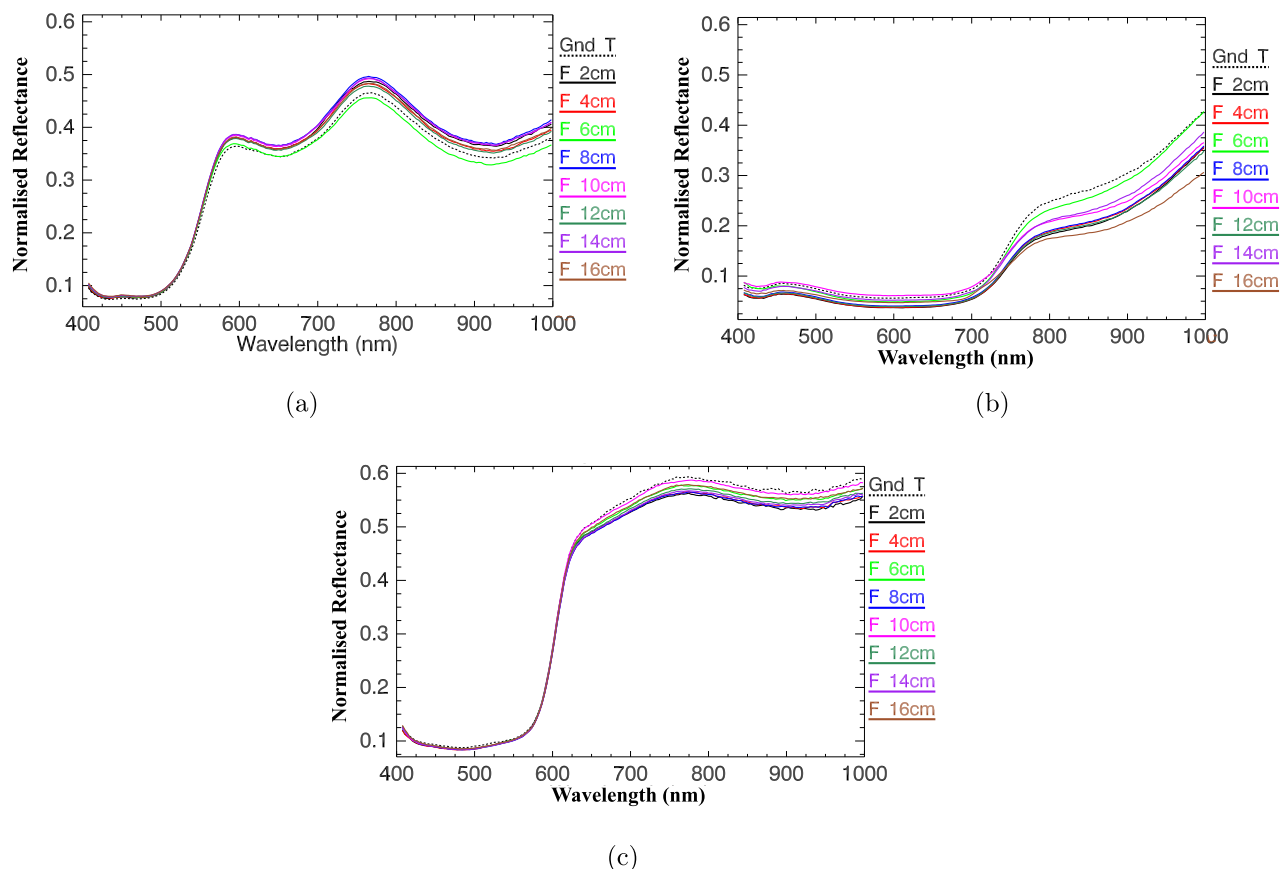


Figure 6. Spectrum for different pigment patch at different focus distance; (a) Patch O, (b) Patch OB, and (c) Patch Vow.

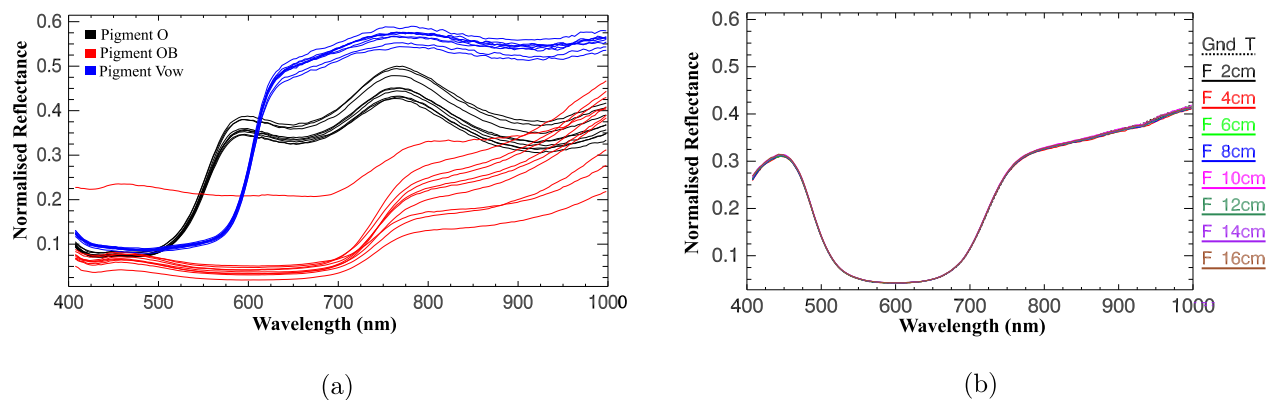


Figure 7. (a) Spectrum for pigment patches obtained at multi-point; for patch O (in black) and patch Vow (in blue), variation is mainly from 550–1000 nm whereas, for patch OB (in red), variation is over the entire wavelength range with slightly higher towards 1000 nm; (b) Spectrum for ColorChecker blue patch (number 23) at the different focus distance.

of two (Fig. 9b), and a mixture of 3 pigments (Fig. 9c). To get a smoother spectral curve, we used a window size of 10×10 pixels i.e., averaging the spectrum over 10 adjacent pixels. It is observed that the change in the spectrum for different SNR levels was lower for all patches over the entire wavelength range. There is no recommendation or standard practice for considering an exact number of pixels to plot the average spectrum. However, experts recommend focusing on a small section of paintings by using between 6 and 18 pixels. When

the size of this window was changed to 1×1 pixel, we notice a variation in spectrum i.e., noisier which decreased with a higher value of N , a result for a patch O is shown in Fig. 9(d). Spectrum is plotted with an offset in normalized reflectance for better visualization.

It can be observed that there is a variation in the spectrum mostly in the regions of 400–500 nm and 850–1000 nm and as SNR increases the spectrum become smoother (less variation). The variation seen is for the reason

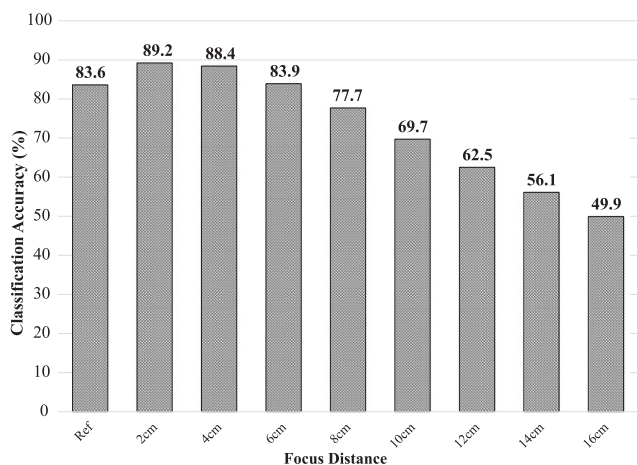


Figure 8. Overall classification accuracy for pigment mockup at the different focus distances.

that exposure in this region requires a longer time compared to mid-region wavelength to overcome the effect of lower quantum energy (sensitivity) of a detector. One possible way to improve this is by using an equalization filter, as it attenuates the light in the mid-region and improves the relative SNR at both ends region of the wavelength range. Figure 10 illustrates the spectrum obtained after using an equalization filter for three patches and the ColorChecker (white patch #24). The spectrum obtained with and without a filter is shown by a solid and dotted line, respectively. It can be seen that, towards both ends of the wavelength range, the spectral variation decreases when the equalization filter is used. The experiment was performed at a distance of 30 cm from the camera to the mockup and this close distance could be one reason for obtaining less noisy data. Classification accuracy for pigment mockup for the different SNRs did not differ much, and the results are shown in Figure 11, there is only a change in obtained value after the second decimal. We also computed the classification accuracy for the ColorChecker, and it was above 99% for all 24 patches, this is because the standard ColorChecker patches have smooth spectral curve characteristics.

4.3 Integration Time

For different integration times, as shown in Figure 12, the magnitude of the spectrum for all three patches did not show any significant changes. A slight shift can be noticed for patches OB (Fig. 12b) and Vow (Fig. 12c) in the range of 800–1000 nm. It implies similar accuracy in HSI data can be obtained with reduced measurement time, i.e., less exposure of an object to radiation. As shown in Fig. 12(d), the spectrum obtained from the ColorChecker for different integration times were also identical. During the acquisition, the illumination intensity varied such that pixels in the field of view have saturation values between 85% and 10%, and the spectrum was plotted by taking an average of 10×10 pixels. However, for the non-homogeneous paintings, neighboring pixels could have different characteristics. Thus, obtaining an average over a bigger window size would not be possible,

so that the result might be affected. The classification accuracy is shown in Figure 13, which illustrates that for the variation in integration time, the classification accuracy is moreover the same. It can also be observed that for variation in either of parameters SNR or integration time, similar classification accuracy can be obtained with sufficient illumination level.

4.4 Illumination

To analyze the effect of illumination angle on the spectral data, the acquisition was done with focused illuminants at three different angles. The result obtained is shown in Figure 14. It illustrates that there is a shift in the spectrum in the range of 600–1000 nm for patch O and Vow, but this is not the case for Vb and OB. The reason for this is assumed to be the non-homogeneity in the surface of pigment patches. It can also be noticed that at an angle of 30° and 45° there is very little variation in the spectrum for all four cases whereas, for O and Vow, there is a slightly high shift in magnitude at 60°. Classification accuracy, as shown in Figure 15, is higher at 45° and changes at a different angle of illumination.

4.5 General Observation

Patches in a pigment mockup are separated from each other, which is not common in real paintings, as elements in the paintings are normally close to each other. Adjacent pixels of different pigments can be misclassified as the spatial resolution changes with focus distance and can change the classification result. A shift in the spectrum does not have any significant effect on the classification accuracy for the attributes SNR and integration time, but this could be important for other applications such as fading or applications that have different concentrations of the same pigment. The influence of SNR and integration time can be more visible if the distance between the camera and object is increased, which could be the case when scanning larger paintings. For larger objects, a rotational stage is used which introduces geometrical errors. An experiment can be conducted in the future to see how this geometrical distortion affects the classification accuracy. Despite having optimal instrumental setup and calibration workflow, pigments surface non-homogeneity in artwork arising from the brushstroke, various thickness layers, compositions in pigments, etc., can affect the obtained data, resulting in misclassification and identification. Further experiments need to be conducted to analyze various factors constituting non-homogeneity on pigment surfaces in works of art, for example, thicknesses, textures, etc. and correlating them with classification accuracy. The mockup in our experiment was unvarnished, usually, paintings are varnished in a real scenario and illumination geometry can cause specular reflection on painting [73]. Berns et al. [74] explained in detail about optics behind varnished paintings, which states that the physical parameters of a varnish affect its optical properties when applied to paintings. Experiments with a new mockup addressing these limitations can be conducted in the future to get a comprehensive result for classification accuracy.

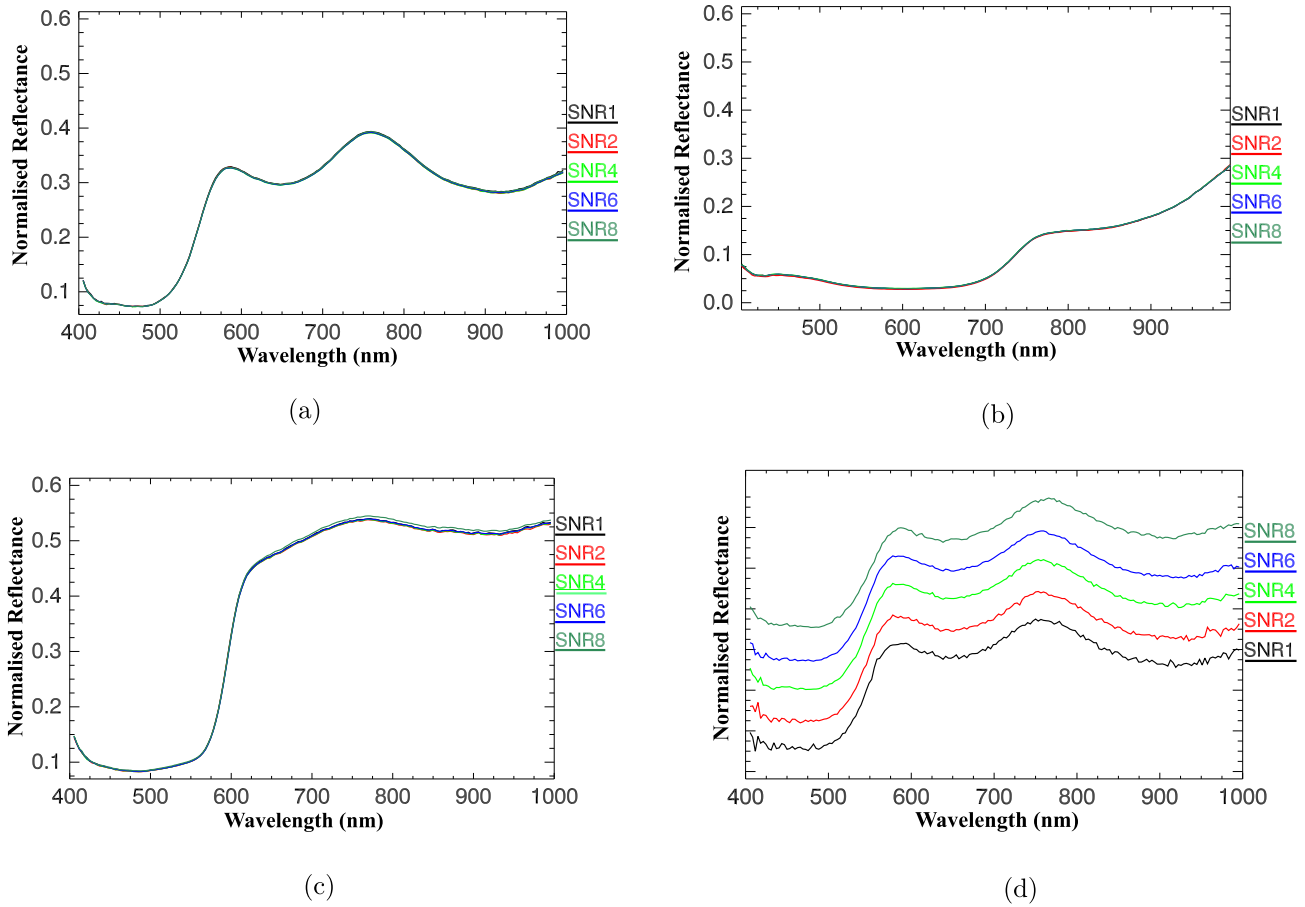


Figure 9. A spectrum of different pigments patch for different SNR; (a) Patch O, (b) Patch OB, (c) Patch Vow, and (d) Spectrum for patch O with offset in the normalized reflectance.

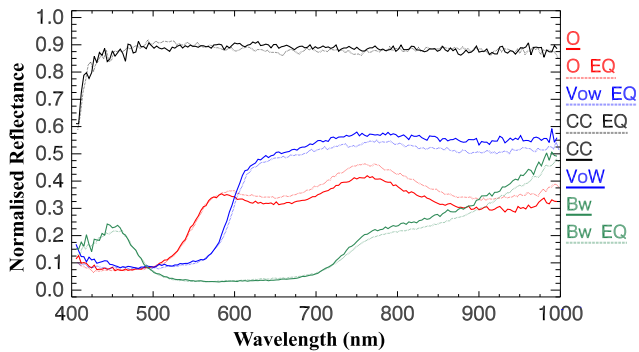


Figure 10. Spectrum for different pigment patches and the ColorChecker: with and without an equalization filter. The letters O, Vow, and Bw represent spectrum for pigment without equalization filter and letter with underscore suffix EQ represents spectrum obtained using the equalization filter.

5. CONCLUSION

Hyperspectral imaging is being used more frequently in the cultural heritage field to study materials and their distribution. The quality of the acquired hyperspectral data is important to produce accurate and reproducible spectral data for the analysis and documentation of a

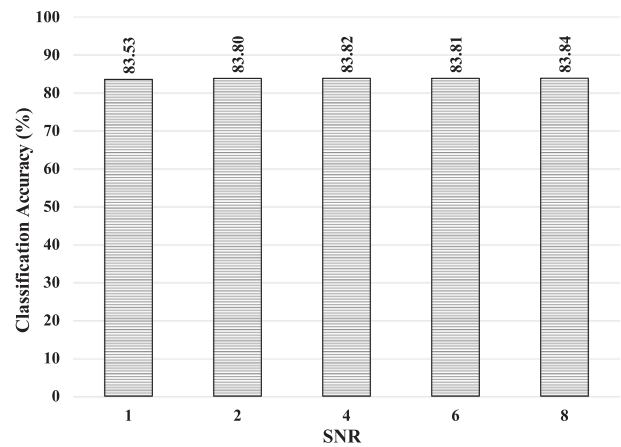


Figure 11. Classification accuracy at different SNR values.

work of art. It can be influenced by different acquisition parameters and is also dependent upon the attributes linked to specific applications. In CH, pigment classification of artwork materials, such as paintings, is of importance for conservators for precise analysis of objects and their historic value. Therefore, to understand how the acquisition

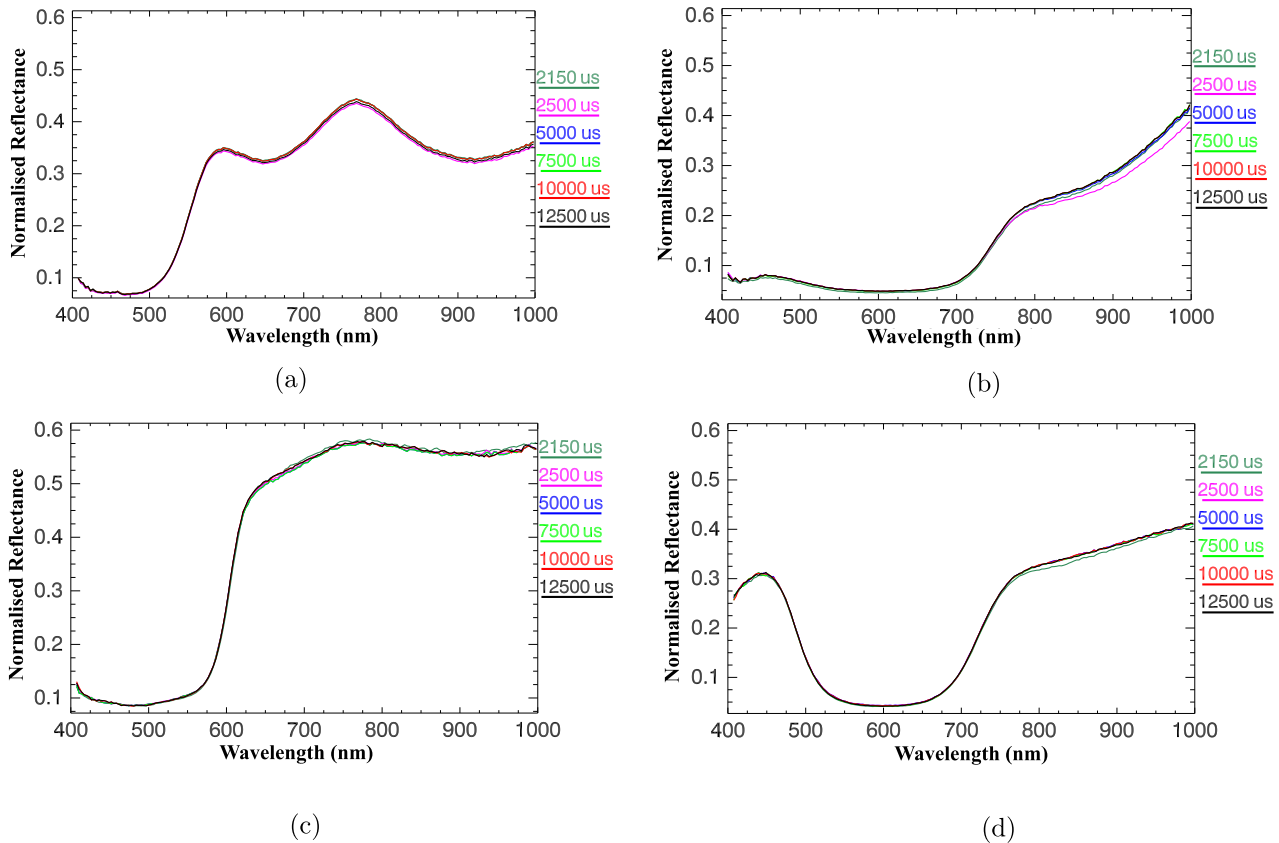


Figure 12. Spectrum for different pigment patches and ColorChecker for different integration time; (a) Patch O, (b) Patch OB, (c) Patch Vow and (d) ColorChecker blue patch (number 23).

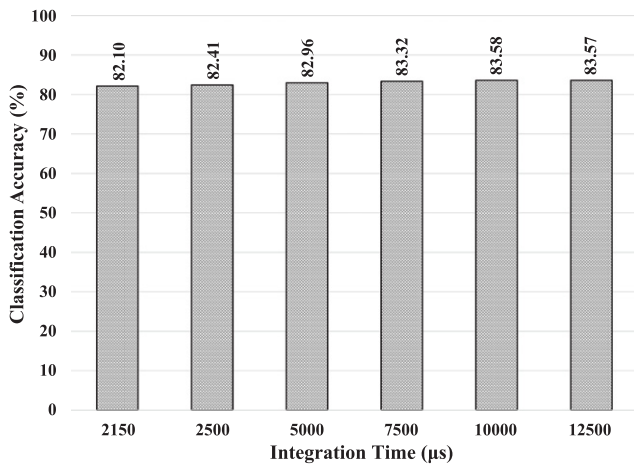


Figure 13. Classification accuracy at different integration time.

parameters affect the quality of the obtained spectral data, we investigated the influence of four key parameters, namely, focus distance, signal-to-noise ratio, integration time, and illumination geometry on pigment classification accuracy for a mockup using hyperspectral imaging in visible and near-infrared regions.

We observed that pigment classification accuracy is influenced by a change in focus distance. Moving an object

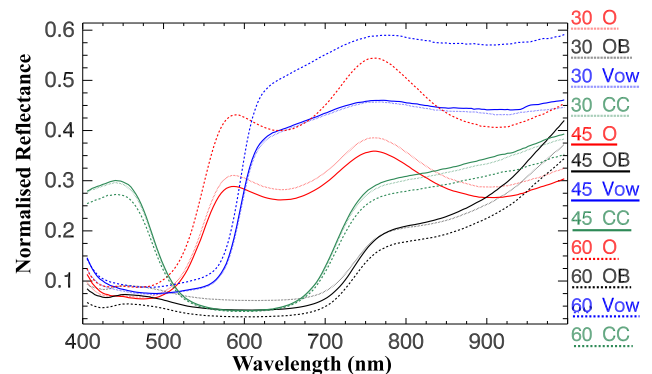


Figure 14. Spectrum for different pigments patches and the ColorChecker at three different illumination angles. The number in the legend represents the angle of illumination.

away from the focus plane, pixels appear out of focus resulting in a blurred image. Blurring acts as a low pass filter and smooths edges and consequently increases the classification accuracy, however, after a certain distance, the classification accuracy starts to decrease. SNR and integration time have less effect over classification compared to focus. One possible reason for this might be due to less noise in a close-range laboratory setup. The pigment patches in the mockup have an uneven surface, which results in

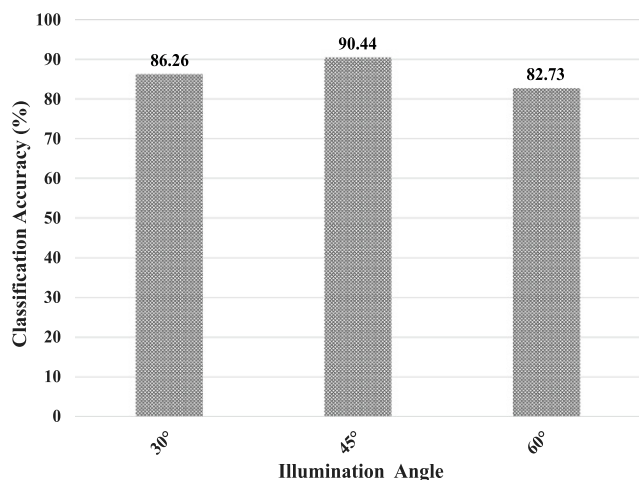


Figure 15. Classification accuracy at a different angle of illumination.

significant variation in the spectrum obtained at different pixels within the same patch. Changing the illumination angle changes the magnitude of the obtained spectrum to some extent and also varies the classification accuracy. An equalization filter can help to reduce the noise in the obtained spectrum especially at two ends of the wavelength range in the VNIR region.

ACKNOWLEDGMENT

This work is carried out at the Norwegian Colour and Visual Computing Laboratory (Colourlab), within the Department of Computer Science (IDI), as part of the CHANGE (Cultural Heritage Analysis for New Generations) project. And has received funding from the European Union's Horizon 2020 research and innovation program under the Marie Skłodowska-Curie grant agreement No. 813789.

REFERENCES

- D. Coulter, P. L. Hauff, and W. L. Kerby, "Airborne hyperspectral remote sensing," *Proc. 5th Decennial Int'l. Conf. on Mineral Exploration* (Decennial Mineral Exploration Conferences, Toronto, Ontario, Canada, 2007), pp. 375–378.
- C.-I. Chang, *Hyperspectral Imaging: Techniques for Spectral Detection and Classification* (Kluwer Academic/Plenum Publishers, Dordrecht, Netherlands, 2003).
- J. M. Amigo and H. Babamoradi, "Saioa Elcoroaristizabal. Hyperspectral image analysis. A tutorial," *Anal. Chim. Acta* **896**, 34–51 (2015).
- F. D. van der Meer, H. M. A. van der Werff, F. J. A. van Ruitenbeek, C. A. Hecker, W. H. Bakker, M. F. Noomen, M. van der Meijde, E. J. M. Carranza, J. B. de Smeth, and T. Woldai, "Multi- and hyperspectral geologic remote sensing: A review," *Int. J. Appl. Earth Observat. Geoinform.* **14**, 112–128 (2012).
- L. M. Dale, A. Thewis, C. Boudry, I. Rotar, P. Dardenne, V. Baeten, and J. A. F. Pierna, "Hyperspectral imaging applications in agriculture and agro-food product quality and safety control: A review," *Appl. Spectrosc. Rev.* **48**, 142–159 (2013).
- G. Lu and B. Fei, "Medical hyperspectral imaging: A review," *J. Biomed. Opt.* **19**, 1–24 (2014).
- G. Edelman, E. Gaston, T. van Leeuwen, P. J. Cullen, and M. C. G. Aalders, "Hyperspectral imaging for non-contact analysis of forensic traces," *Forensic Sci. Int.* **223**, 28–39 (2012).
- Q. Li, X. He, Y. Wang, H. Liu, D. Xu, and F. Guo, "Review of spectral imaging technology in biomedical engineering: achievements and challenges," *J. Biomed. Opt.* **18**, 1–29 (2013).
- C. Fischer and I. Kakoulli, "Multispectral and hyperspectral imaging technologies in conservation: current research and potential applications," *Stud. Conserv.* **51**, 3–16 (2006).
- G. Shaw and D. Manolakis, "Signal processing for hyperspectral image exploitation," *IEEE Signal Process. Mag.* **19**, 12–16 (2002).
- F. G. France, "Advanced spectral imaging for noninvasive microanalysis of cultural heritage materials: Review of application to documents in the U.S. library of congress," *Appl. Spectrosc.* **65**, 565–574 (2011). PMID: 21639977.
- C. Cucci, J. K. Delaney, and M. Picollo, "Reflectance hyperspectral imaging for investigation of works of art: old master paintings and illuminated manuscripts," *Acc. Chem. Res.* **49**, 2070–2079 (2016).
- R. Mayer, *The Painter's Craft: An Introduction to Artists' Methods and Materials*, Studio Book (Van Nostrand, New York, NY, 1966).
- B. H. Stuart, "Conservation materials," *Analytical Techniques in Materials Conservation* (John Wiley & Sons, Ltd., 2007), Chapter 1, pp. 1–42.
- D. Bai, D. W. Messinger, and D. Howell, "Hyperspectral analysis of cultural heritage artifacts: pigment material diversity in the Gough Map of Britain," *Opt. Eng.* **56**, 1–11 (2017).
- M. Picollo, C. Cucci, A. Casini, and L. Stefani, "Hyper-spectral imaging technique in the cultural heritage field: New possible scenarios," *Sensors* **20**, 2843 (2020).
- S. George, J. Y. Hardeberg, J. Linhares, L. Macdonald, C. Montagner, S. Nascimento, M. Picollo, R. Pillay, T. Vitorino, and E. Keats Webb, "A study of spectral imaging acquisition and processing for cultural heritage," *Digital Techniques for Documenting and Preserving Cultural Heritage* (Amsterdam University Press, Amsterdam, 2019), pp. 141–158.
- D. Foster and K. Amano, "Hyperspectral imaging in color vision research: Tutorial," *J. Opt. Soc. Am. A* **36**, 606 (2019).
- Z. Wang, A. Bovik, H. Sheikh, and E. Simoncelli, "Image quality assessment: From error visibility to structural similarity," *IEEE Trans. Image Process.* **13**, 600–612 (2004).
- P. G. Engeldrum, "A theory of image quality: The image quality circle," *J. Imaging Sci. Technol.* **48**, 447–457 (2004).
- A. Fryskowska and J. Stachelek, "A no-reference method of geometric content quality analysis of 3D models generated from laser scanning point clouds for hBIM," *J. Cultural Heritage* **34**, 95–108 (2018). Technoheritage 2017.
- E. Christophe, D. Léger, and C. Mailhes, "Quality criteria benchmark for hyperspectral imagery," *IEEE Trans. Geosci. Remote Sensing* **43**, 2103–2114 (2005).
- B.-C. Gao, C. Davis, and A. Goetz, "A review of atmospheric correction techniques for hyperspectral remote sensing of land surfaces and ocean color," *2006 IEEE Int'l. Symposium on Geoscience and Remote Sensing* (IEEE, Piscataway, NJ, 2006), pp. 1979–1981.
- R. Pillay, J. Hardeberg, and S. George, "Hyperspectral imaging of art: Acquisition and calibration workflows," *J. Am. Inst. Conservat.* **58**, 3–15 (2019).
- M. Kubik, "Chapter 5 hyperspectral imaging: A new technique for the non-invasive study of artworks," in *Physical Techniques in the Study of Art, Archaeology and Cultural Heritage*, edited by D. Creagh and D. Bradley (Elsevier, Amsterdam, Netherlands, 2007), Vol. 2, pp. 199–259.
- J. A. Toque, M. Komori, Y. Murayama, and A. Ide-Ektessabi, "Analytical imaging of traditional Japanese paintings using multispectral images," *Int'l. Conf. on Computer Vision, Imaging and Computer Graphics* (Springer, Berlin/Heidelberg, 2009), pp. 119–132.
- C. Relf, *Image Acquisition and Processing with LabVIEW*. 07 2003.
- M. W. Burke, *Image Acquisition: Handbook of Machine Vision Engineering: Volume 1* (Elsevier, Amsterdam, Netherlands, 1996).
- S. Ray, "Chapter 6 – photographic and geometrical optics," in *The Manual of Photography*, edited by E. Allen and S. Triantaphillidou (Focal Press, Oxford, 2011), pp. 103–117.
- E. Webb, S. Robson, and R. Evans, "Quantifying depth of field and sharpness for image-based 3D reconstruction of heritage objects," *ISPRS – Int'l. Archives of the Photogrammetry, Remote Sensing and Spatial Information Sciences XLIII-B2-2020*, 911–918 (2020).
- K. Martinez and A. Hamber, "Towards a colorimetric digital image archive for the visual arts," *Proc. SPIE* **1073**, 114–121 (1989).
- S. Lorusso, A. Natali, and C. Matteucci, "Colorimetry applied to the field of cultural heritage: examples of study cases," *Conservation Science in Cultural Heritage 1974-4951* **7**, 187–208 (2007).

- 33 P. Korytkowski and A. Olejnik-Krugly, "Precise capture of colors in cultural heritage digitization," *Color Res. Appl.* **42**, 333–336 (2017).
- 34 E. Franceschi, P. Letardi, and G. Luciano, "Colour measurements on patinas and coating system for outdoor bronze monuments," *J. Cultural Heritage* **7**, 166–170 (2006).
- 35 M. Bacci, "Optical spectroscopy and colorimetry," *Proc. Int'l. School of Physics Enrico Fermi* (IOS Press, Ohmsha, 1999, 2004), Vol. 154, pp. 1–16.
- 36 R. Fontana, A. D. Fovo, J. Striova, L. Pezzati, E. Pampaloni, M. Raffaelli, and M. Barucci, "Application of non-invasive optical monitoring methodologies to follow and record painting cleaning processes," *Appl. Phys. A* **121**, 957–966 (2015).
- 37 S. Legrand, F. Vanmeert, G. Van der Snickt, M. Alfeld, W. De Nolf, J. Dik, and K. Janssens, "Examination of historical paintings by state-of-the-art hyperspectral imaging methods: From scanning infra-red spectroscopy to computed x-ray laminography," *Heritage Sci.* **2**, 13 (2014).
- 38 H. Liang, "Advances in multispectral and hyperspectral imaging for archaeology and art conservation," *Appl. Phys. A: Mater. Sci. Process.* **106**, 309–323 (2012).
- 39 T. Vitorino, A. Casini, C. Cucci, A. Gebejesje, J. Hiltunen, M. Hauta-Kasari, M. Picollo, and L. Stefani, "Accuracy in colour reproduction: Using a colorchecker chart to assess the usefulness and comparability of data acquired with two hyper-spectral systems," *Computational Color Imaging* (Springer International Publishing, Cham, 2015), pp. 225–235.
- 40 F. Daniel, A. Mounier, J. Pérez-Arantegui, C. Pardos, N. Prieto-Taboada, S. Fdez-Ortiz de Vallejuelo, and K. Castro, "Hyperspectral imaging applied to the analysis of goya paintings in the museum of Zaragoza (Spain)," *Microchem. J.* **126**, 113–120 (2016).
- 41 R. Qureshi, M. Uzair, K. Khurshid, and H. Yan, "Hyperspectral document image processing: Applications, challenges and future prospects," *Pattern Recognit.* **90**, 12–22 (2019).
- 42 P. Geladi, J. Burger, and T. Lestander, "Hyperspectral imaging: calibration problems and solutions," *Chemo Metr. Intell. Lab. Syst.* **72**, 209–217 (2004). *Advances in Chromatography and Electrophoresis – Conferentia Chemometrica 2003*, Budapest.
- 43 J. Qin, "Chapter 5 – hyperspectral imaging instruments," in *Hyperspectral Imaging for Food Quality Analysis and Control*, edited by D.-W. Sun (Academic Press, San Diego, 2010), pp. 129–172.
- 44 L. W. MacDonald, T. Vitorino, M. Picollo, R. Pillay, M. Obarzanowski, J. Sobczyk, S. Nascimento, and J. Linhares, "Assessment of multispectral and hyperspectral imaging systems for digitisation of a Russian icon," *Heritage Sci.* **5**, 1 (2017).
- 45 T. R. Peery and D. W. Messenger, "Spatial resolution as a trade-space for low-light imaging of sensitive cultural heritage documents," *J. Cultural Heritage* **45**, 81–90 (2020).
- 46 British Standards Institution. *PAS 198: 2012: Specifications for Managing Environmental Conditions for Cultural Collections* (BSI Standards, London, 2012).
- 47 Illuminating Engineering Society and Illuminating Engineering Society of North America. *Recommended Practice for Museum Lighting: ANSI/IES RP-30-17*. ANSI/IES (Illuminating Engineering Society of North America, New York, 2017).
- 48 Still Image Working Group. Technical guidelines for digitizing cultural heritage materials. Technical Report, Federal Agencies Digitization Guidelines Initiative (September 2016).
- 49 D. Saunders and J. Kirby, "Light-induced damage: investigating the reciprocity principle," *11th Triennial Meeting, Edinburgh, Scotland, 1–6 September, 1996: Preprints* (ICOM Committee for Conservation, Paris, France, 1996), pp. 87–90.
- 50 R. Whetton, T. Waine, and A. Mouazen, "Optimising configuration of a hyperspectral imager for on-line field measurement of wheat canopy," *Biosyst. Eng.* **155**, 84–95 (2017).
- 51 N.-N. Wang, D.-W. Sun, Y.-C. Yang, H. Pu, and Z. Zhu, "Recent advances in the application of hyperspectral imaging for evaluating fruit quality," *Food Anal. Methods* **9**, 178–191 (2015).
- 52 A. Hayem-Ghez, E. Ravaud, C. Boust, G. Bastian, M. Menu, and N. Brodie-Linder, "Characterizing pigments with hyperspectral imaging variable false-color composites," *Appl. Phys. A* **121**, 939–947 (2015).
- 53 F. Grillini, J. Thomas, and S. George, "Linear, subtractive and logarithmic optical mixing models in oil painting," *Colour Visual Comput. Symp.* (CEUR-WS.org, Gjøvik, Norway, 2020), Vol. 2688.
- 54 I. Sandu, M. Sá, and M. Pereira, "Ancient "gilded" art objects from european cultural heritage: A review on different scales of characterization," *Surf. Interface Anal.* **43**, 1134–1151 (2011).
- 55 T. Cavaleri, A. Giovagnoli, and M. Nervo, "Pigments and mixtures identification by visible reflectance spectroscopy," *Proc. Chem.* **8**, 45–54 (2013). *YOUTH in the CONSERVATION OF CULTURAL HERITAGE, YOCOCU 2012*.
- 56 R. J. H. Clark, "Pigment identification on medieval manuscripts by Raman microscopy," *J. Molecular Struct.* **347**, 417–427 (1995). *Molecular Spectroscopy and Molecular Structure*, 1994.
- 57 J. Delaney, E. Walmsley, B. Berrie, and C. Fletcher, "Multispectral imaging of paintings in the infrared to detect and map blue pigments," *Scientific Examination of Art: Modern Techniques in Conservation and Analysis* (The National Academies Press, Washington, DC, 2005), pp. 120–136.
- 58 H. Deborah, S. George, and J. Y. Hardeberg, "Pigment mapping of the scream (1893) based on hyperspectral imaging," *Int'l. Conf. on Image and Signal Processing* (Springer, Cham, 2014), Vol. 8509, pp. 247–256.
- 59 C. Balas, G. Epitropou, A. Tsapras, and N. Hadjinicolaou, "Hyperspectral imaging and spectral classification for pigment identification and mapping in paintings by El Greco and his workshop," *Multimedia Tools Appl.* **77**, 9737–9751 (2018).
- 60 L. Tan and M.-I. Hou, "A study on the application of SAM classification algorithm in seal of calligraphy and painting based on hyperspectral technology," *2016 4th Int'l. Workshop on Earth Observation and Remote Sensing Applications (EORS)* (IEEE, Piscataway, NJ, 2016), pp. 415–418.
- 61 C. Cucci, A. Casini, L. Stefani, M. Picollo, and J. Jussila, "Bridging research with innovative products: a compact hyperspectral camera for investigating artworks: a feasibility study," *Proc. SPIE* **10331**, 1033106 (2017).
- 62 O. A. De Carvalho and P. R. Meneses, "Spectral correlation mapper (SCM): an improvement on the spectral angle mapper (SAM)," *Summaries of the 9th JPL Airborne Earth Science Workshop, JPL Publication 00-18* (JPL Publication, Pasadena, CA, 2000), Vol. 9.
- 63 H. Z. Mohd Shafri, A. Suhaili, and S. Mansor, "The performance of maximum likelihood, spectral angle mapper, neural network and decision tree classifiers in hyperspectral image analysis," *J. Comput. Sci.* **3**, 419–423 (2007).
- 64 C.-I. Chang, "An information-theoretic approach to spectral variability, similarity, and discrimination for hyperspectral image analysis," *IEEE Trans. Inform. Theory* **46**, 1927–1932 (2000).
- 65 E. Angelopoulou, S. Lee, and R. Bajcsy, "Spectral gradient: a material descriptor invariant to geometry and incident illumination," *Proc. Seventh IEEE Int'l. Conf. on Computer Vision* (IEEE, Piscataway, NJ, 1999), Vol. 2, pp. 861–867.
- 66 Norsk Elektro Optikk. <http://www.hyspex.no/>. Accessed: 20 December 2020.
- 67 Spectralon® Multi-step Targets. <https://www.labspherestore.com/product-p/aa-006xx-000.htm>. Accessed: 11 September 2020.
- 68 X-Rite ColorChecker Classic. <https://www.xrite.com/>. Accessed: 11 September 2020.
- 69 D. Saunders and J. Cupitt, "Image processing at the national gallery: The vasari project," *National Gallery Technical Bulletin* **14**, 72–85 (1993).
- 70 Welcome to Spectral Python (SPy). <http://www.spectralpython.net>.
- 71 M. Sokolova and G. Lapalme, "A systematic analysis of performance measures for classification tasks," *Inform. Process. Manage.* **45**, 427–437 (2009).
- 72 J. Lever, M. Krzywinski, and N. Altman, "Points of significance: Classification evaluation," *Nat. Methods* **13**, 603–604 (2016).
- 73 D. C. Day, Technical report: Evaluation of optical flare and its effects on spectral estimation accuracy. pp. 1–19, 2003. Accessed: 20 December 2020.
- 74 R. S. Berns and E. R. de la Rie, "Exploring the optical properties of picture varnishes using imaging techniques," *Stud. Conserv.* **48**, 73–82 (2003).